Acta of Bioengineering and Biomechanics
Vol. 25, No. 2, 2023

Original paper
DOI: 10.37190/ABB-02244-2023-04

Finite element analysis on pushing the molar backwards using invisible aligner with different migration displacement

JIWU ZHANG[1], LILI MA[2], YUZHONGXIU REN[3], YUQING ZHOU[1], RONG WEI[4], QIGUO RONG[1]*

[1] Department of Mechanics and Engineering Science, College of Engineering, Peking University, Beijing, China.
[2] Center of Stomatology, China Japan Friendship Hospital, Beijing, China.
[3] Department of Stomatology, The Fifth Affiliated Hospital of Sun Yat-sen University, Zhuhai, China.
[4] Peking University Academy for Advanced Interdisciplinary Studies, Beijing, China.

Purpose: This paper examines the biomechanical mechanism behind the effect of the invisible aligner technique on tooth movement processes. *Methods*: To compare the effects of different target positions on tooth movement and the periodontal ligament (PDL), two kinds of aligners were designed to provide displacements of 0.2 mm (Model A) and 0.3 mm (Model B). Different displacements of the maxillary second molar were simulated using the finite element (FE) method. *Results*: The results of numerical simulations showed that the maximum stress was in the PDL of the distal surface and the palatal surface. The stress of the PDL in Model B was larger than Model A, with the displacement of the second molar 0.027 mm in Model A, by 44.9% lesser than that in Model B. *Conclusions*: The aligner that provided a displacement of 0.2 mm was more suitable for pushing the second molar backward in the initial stage. During the tooth movement processes, the displacement of the crown was larger than that of the root and the displacement decreased gradually from the crown to the root. In addition, the displacement and rotation of teeth during orthodontic treatment were measured and analysed.

Key words: *invisible aligner, finite element analysis, orthodontic tooth movement, periodontal ligament*

1. Introduction

With the development of 3D scanning technology, dentists can use computer techniques to observe and measure patients' teeth. A new type of invisible aligner technique was introduced in the late 1990s. It combines visualization 3D image processing and laser rapid prototyping technology. When using this technology, it is particularly necessary to control tooth movement by an appropriate appliance design and three-dimensional models of each orthodontic stage are processed by rapid laser forming. These aligners can achieve orthodontic treatment through continuous small-scale effects on teeth. Because of the comfort, beauty, detachability and predictability of the effect, the invisible aligners are favoured by orthodontists and adult patients [22], [31], [34], [36]. However, although few clinical studies have been published, no insights into the biomechanics of these aligners regarding tooth movement are available.

The working principles of the invisible and traditional bracket systems differ with respect to the shapes of the aligner and crown. The invisible aligner applies force to deform and produce a reaction force on the crown [2], [8], [14]. The orthodontic force system is more complex for the invisible aligner than the traditional bracket system because the applied force of the invisible aligner does not act on a certain point [20].

The studies indicate that the periodontal ligament (PDL) plays a role in bone remodelling during orthodontic tooth movement [21]. The PDL is a fibrous connective tissue derived from the dental follicle. PDL connects the cementum to alveolar bone and maintains the root of the tooth in the alveolar socket. The suggestion that mandibular remodelling may be controlled by

* Corresponding author: Qiguo Rong, Department of Mechanics and Engineering Science, College of Engineering, Peking University, Beijing 100871. China. E-mail: qrong@pku.edu.cn
Received: April 30th, 2023
Accepted for publication: September 25th, 2023

the PDL has attracted increasing interest in the stress and strain distributions throughout the mandible [3]. The PDL fibres are compressed on the side to which the tooth is pushed and stretched on the opposite side. It is important to include the fibres of the PDL in finite element (FE) models when investigating orthodontic tooth movement.

Due to the sequential nature of the orthodontic treatment, the second molar, the outermost molar, is considered the most critical step in the orthodontic process. This study aimed to investigate the mechanics of tooth movement produced by an aligner, especially for the effects of orthodontic design on bodily movement. In addition, this paper also discusses the stress distribution of the appliance under different migration displacements and the stress magnitude and direction of the PDL to quantitatively evaluate the response to different displacements. To achieve this goal, FE models were used to evaluate the orthodontic distalization movement of a second maxillary molar by aligners, different displacements were analysed.

2. Materials and methods

All experiments were approved by the Ethics Committee of Drugs (Device) of China-Japan Friendship Hospital. The imaging data obtained from the database were CT scans of the head with complete dentition, normal tooth and root anatomy, using a 256-Slice scanner (LightSpeed VCT, GE, USA). Images were reconstructed on a 512 × 512 pixel matrix at 0.5 mm thickness. The digital imaging and communications in medicine files of CT scans were transferred to the interactive medical image control system Mimics 17.0 (MIMICS, Materialise, Belgium) to reconstruct the maxilla and teeth (from the maxillary left central incisor to the left second molar) based on the different grayscale values. Data selection was performed on the intersection of teeth and maxilla. The data of teeth and maxilla were imported into SolidWorks 2016 (SolidWorks, Concord, Massachusetts, USA) for data repair. Assuming a uniform thickness of 0.25 mm of PDL, the PDL data was established by extending outward along the normal by 0.25 mm, which was within the average range of PDL thickness [15]–[17], [25], [26]. The data of all the left dentition, PDL and jawbone were replicated using a median mirror to establish three-dimensional data including tooth, PDL and maxillary. In order to create more space for other teeth in the subsequent treatment, the second molar is also the most important initial stage in the orthodontic process compared to other teeth. Therefore, this article simulates the orthodontic treatment of the second molar. To compare the effects of different displacements on tooth movement and the PDL, two kinds of invisible aligners were made and fitted into the target positions for displacements of 0.2 and 0.3 mm as shown in Fig. 1. The dentition groups were named Model A and Model B. The models in this study were calculated using ABAQUS software. Each tooth was not separated into different components and was modelled entirely as dentin. This simplification has been used in previous studies [6], [11], [12]. The tooth, PDL and bone were all assumed to be homogeneous, isotropic and linear elastic materials [24], [27], [30], [33]. The mechanical properties of the models were assigned on the basis of previous studies (Table 1) [5], [28], [29].

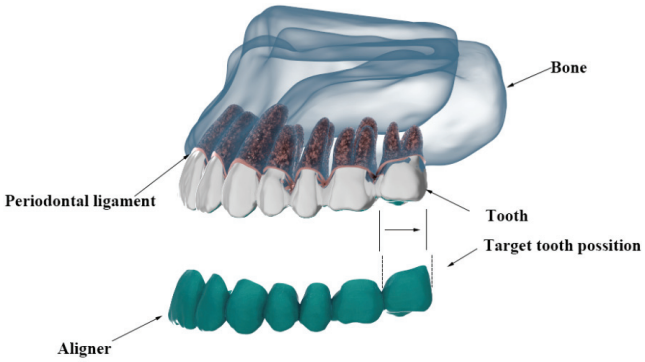

Fig. 1. Diagram of the use of an invisible appliance to push a molar backwards

Table 1. Material properties used in the FEA models

Model	Young's modulus [MPa]	Poisson's ratio
Maxillary bone	13700	0.30
PDL	0.68	0.49
Tooth	18600	0.31
Aligner	816.31	0.30

The interface between the bone and the aligner was modelled as surface-to-surface contact with a friction coefficient of 0.2 [7], [10]. The tooth, PDL and bone were meshed with tetrahedral solid elements, as these elements were well suited to irregular mesh and complex geometries. The aligner was meshed with 4-node shell elements. To achieve satisfactory convergence of the numerical simulation, the FE meshes of the models were sufficiently dense, as shown in Fig. 2.

The numbers of elements and nodes are shown in Table 2. Because of the contact relationship between the invisible calibrator and the teeth, the actual positions of the invisible calibrator and the teeth penetrated each other at the second molar to solve the position relationship of mutual penetration. The teeth

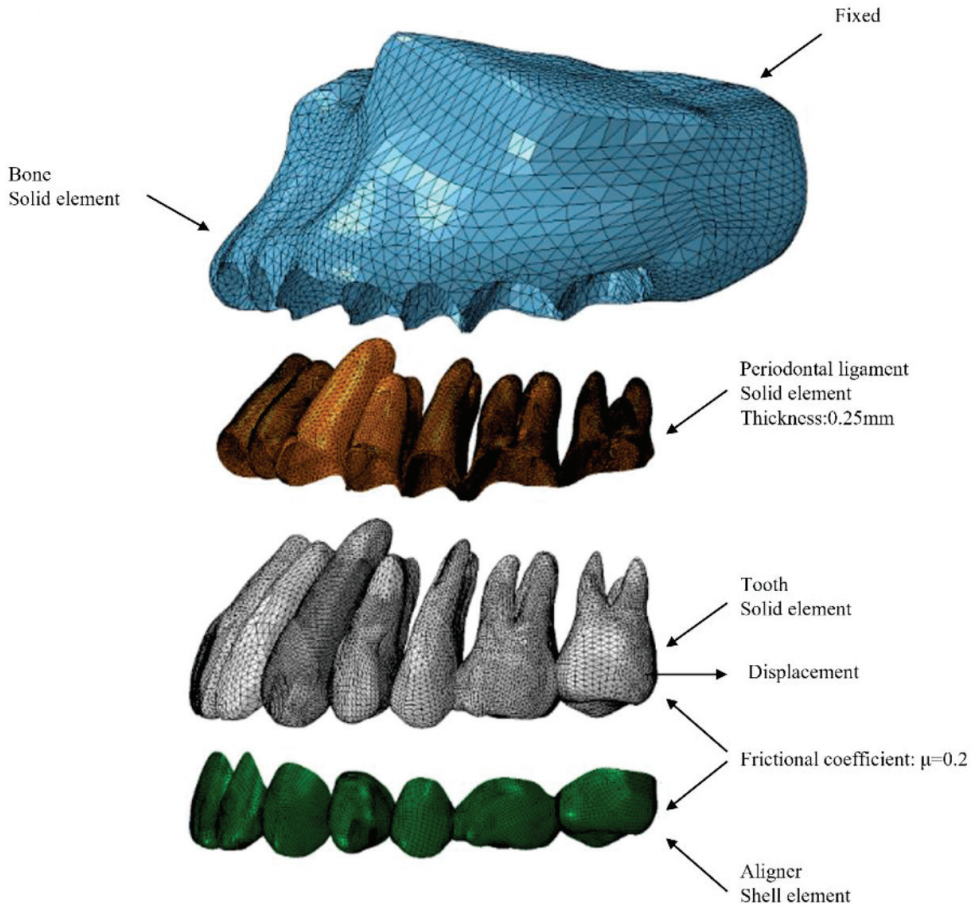

Fig. 2. Finite element model of the invisible aligner

slowly moved in the direction required by the invisible calibrator. Therefore, it was unnecessary to apply boundary conditions other than alveolar bone fixation to simulate the effect of the invisible aligner. This was achieved by prescribing a displacement vector at the invisible aligner. This process was completely consistent with patients wearing aligners [4].

Table 2. Number of elements and nodes in the FEA models

	Elements	Nodes
Maxillary bone	231304	45434
PDL	155360	49085
Tooth	329514	66600
Aligner of Model A	7192	7199
Aligner of Model B	13315	13409

3. Results

The stress of the PDL

As shown in Fig. 3, the maximum von Mises stress in the PDL of Model A was 34.9 kPa, which was by 113.8% larger than that of Model B (Table 3). The stress contours showed that stress concentration occurred on the PDL of the maxillary second and first molar teeth.

Table 3. Maximum von Mises stress of the PDL [kPa]

	Model A	Model B
First molar PDL	19.50	40.43
Second molar PDL	35.55	49.25

The maximum and minimum principal stresses of the two invisible aligner types, including the first molar PDL and the second molar PDL, were compared in our study (Fig. 4, Tables 4 and 5). For invisible aligner loading, compressive behaviour dominated PDL resistance against tooth movement, and tensile and compressive behaviour were more profound. The maximum values of the principal stresses in the second molar PDL were 0.74 MPa compressive and 0.64 MPa tensile for 0.2 mm invisible aligner loading. For 0.3 mm invisible aligner loading, the maximum values of the principal stress in the second molar PDL were 1.23 MPa compressive and 1.03 MPa tensile.

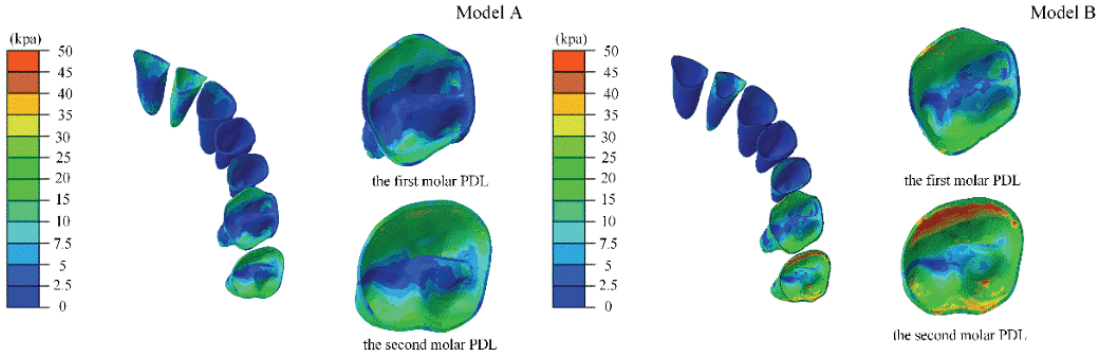

Fig. 3. The von Mises stress in the PDL immediately after placement
(Model A: The invisible aligner for 0.2 mm displacement, Model B: The invisible aligner for 0.3 mm displacement)

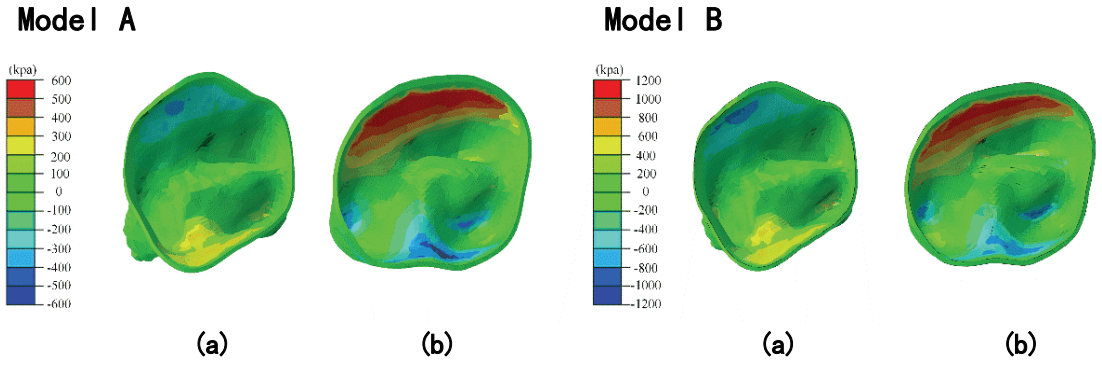

Fig. 4-1. The maximum principal stress of the first and the second molars
(Model A: The invisible aligner with 0.2 mm displacement; Model B: The invisible aligner with 0.3 mm displacement;
(a) the first molar, (b) the second molar)

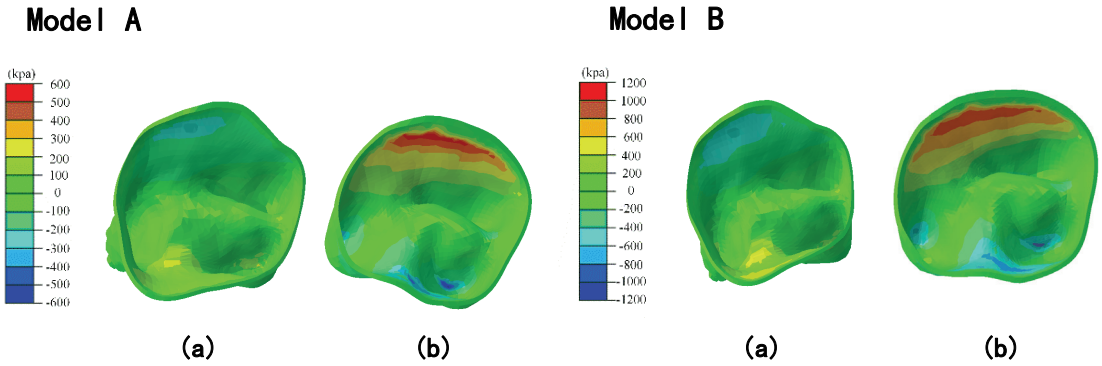

Fig. 4-2. The minimum principal stress of the first and the second molars
(Model A: The invisible aligner for 0.2 mm displacement; Model B: The invisible aligner for 0.3 mm displacement;
(a) the first molar, (b) the second molar)

Table 4. The maximum principal stress of the PDL [MPa]

	Model A	Model B
First molar PDL	0.62	0.86
Second molar PDL	0.74	1.23

Table 5. The minimum principal stress of the PDL [MPa]

	Model A	Model B
First molar PDL	0.53	0.96
Second molar PDL	0.64	1.03

Tooth movement under invisible aligners

When pushing the molar backward, only the maxillary first and second molars were considered in this study. The movement of the central incisor immediately after placement of the aligner is shown in Fig. 5. The displacement of the crown was larger than that of the root, and the displacement decreased gradually from the crown to the root. The maximum displacements were 0.027 mm in Model A and 0.049 mm in Model B. In the two models, the displacement and rotation about the centre of the tooth were calculated in three directions. Therefore, the rotation of four teeth and their displacements in three directions were compared in our study (Fig. 5, Table 6).

Table 6. Maximum rotational angles of teeth

	Model A		Model B	
	First molar	Second molar	First molar	Second molar
Rotational angles around the *X*-axis	0.04	0.13	0.05	0.22
Rotational angles around the *Y*-axis	0	0.03	0.01	0.01
Rotational angles around the *Z*-axis	0.01	0.08	0.02	0.26

Regarding the tooth local coordinate system, the *X*-axis represented the sagittal plane in the maxilla direction, the *Y*-axis was pointed in the backward direction and the *Z*-axis corresponded to the direction perpendicular to the *XY*-plane. They represent rotation in the

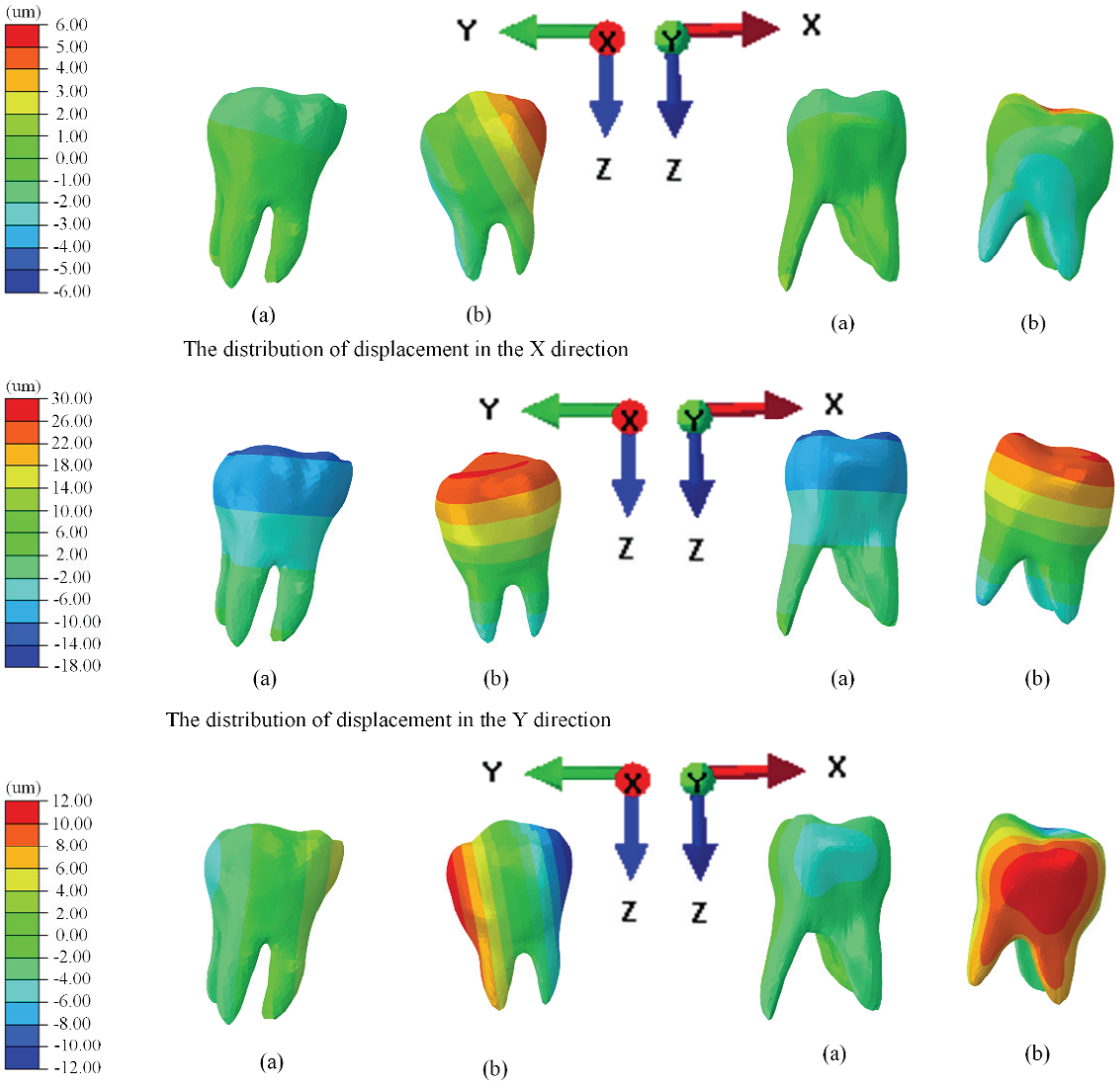

Fig. 5-1. The distributions of displacement for Model A in the *X*-, *Y*-, and *Z*-directions ((a) the first molar, (b) the second molar)

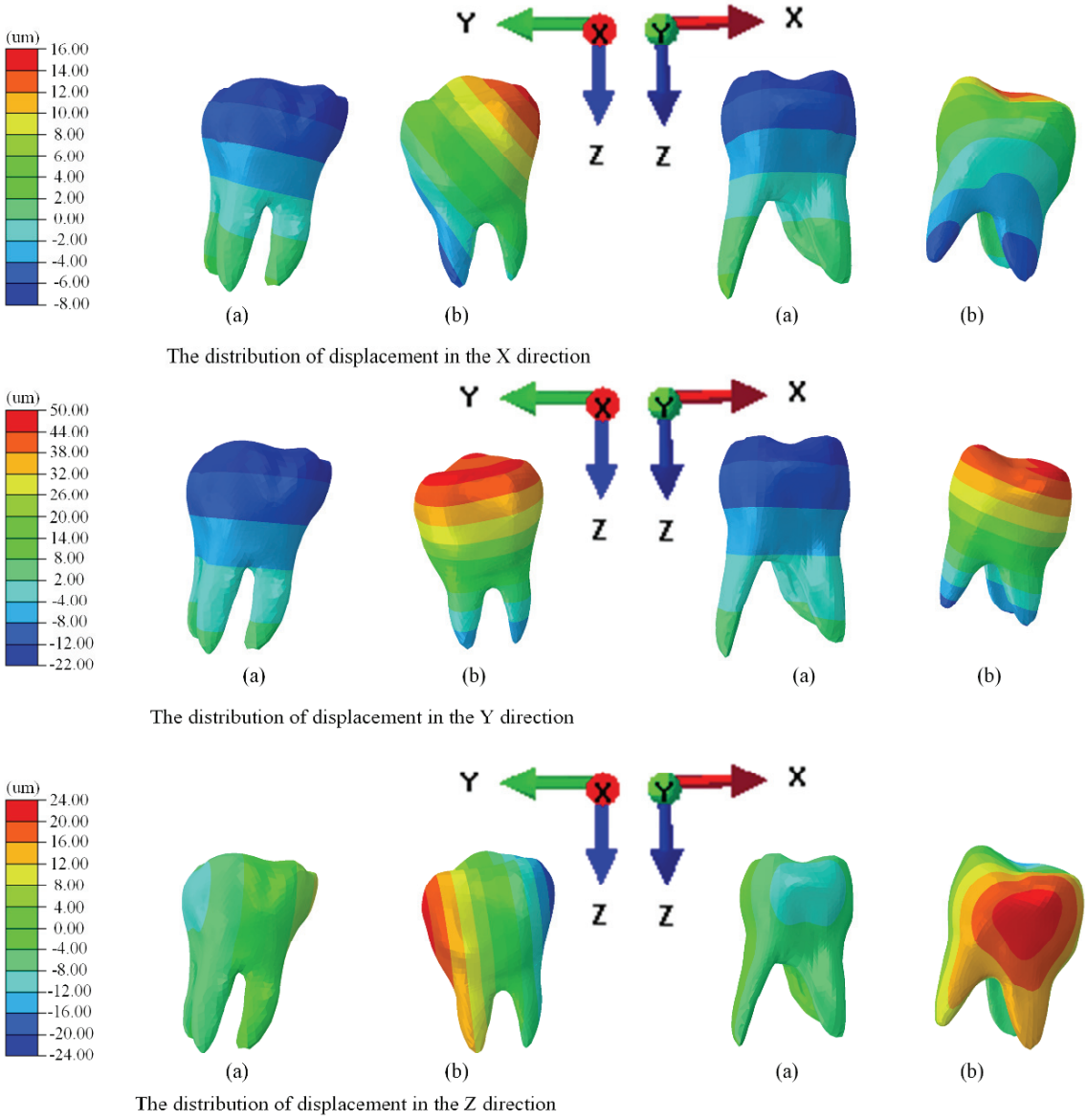

Fig. 5-2. The distributions of displacements for Model B in the *X*-, *Y*-, and *Z*-directions ((a) the first molar, (b): the second molar)

direction of tooth migration, lingual buccal rotation and tooth rotation, respectively. The displacement of the tooth was smaller in Model A than in Model B. In the aligner with migration displacement of 0.2 mm, the rotational angles of the second molar around the *X*-, *Y*-, and *Z*-axes were 0.13°, 0.03°, and 0.08°, respectively (Fig. 5-1). In the aligner with a migration displacement of 0.3 mm, the rotational angles of the second molar around the *X*-, *Y*-, and *Z*-axes were 0.22°, 0.01° and 0.26°, respectively (Fig. 5-2).

The equivalent stress of the aligner

The stress distributions of the Model A and Model B aligners were similar, as shown in Fig. 6. The stress concentration regions of both models were located in the junction regions of the aligners. The maximum von Mises stress was larger in Model B than Model A.

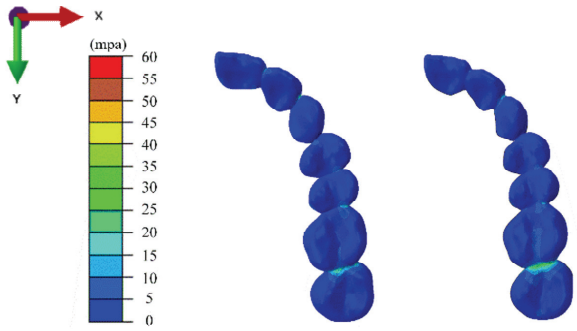

Fig. 6. The principal stresses of the aligners (Model A: The invisible aligner for 0.2 mm displacement, Model B: The invisible aligner for 0.3 mm displacement)

They were 134.2 MPa in Model A and 156.2 MPa in Model B.

4. Discussion

The stress distributions in the different invisible aligners were similar, but their magnitudes differed. The action of stress was observed mostly on the lingual-cervical and labial-cervical sides of the teeth.

Behaviour of the PDL

In this study, different migration displacements of the invisible aligner could cause different biomechanical effects on the PDL regions and tooth movement. The PDL exerted force only where the surrounding bone was under tension, not under compression. Therefore, the PDL provided little resistance to tooth movement in the direction of the applied force and thus transferred negligible loads to the alveolar bone on that side. Conversely, the PDL was stretched on the opposite side and thus, the applied load was essentially transferred there. The following theory was used to explain orthodontic tooth movement: loading of the alveolar wall caused bone resorption, while the load exerted by the stretched PDL on the opposite side caused bone formation [23].

According to the literature [13], tooth movement was determined by pressure on the root surface. The maximum stress value of the PDL should be less than 26 kPa, otherwise, it would cause irreversible necrosis of PDL tissue. Hohmann [18], [19] believed that when the hydrostatic pressure of the PDL capillaries exceeds 4.7 kPa, the risk of root absorption is greatly increased. In this experiment, when the invisible aligner moved 0.2 mm away from the molar, the stress values of all PDL were less than the maximum stress value that the PDL could bear (26 kPa), and there was no significant irreversible damage to the PDL. However, the stress of some PDL was greater than 4.7 kPa, which indicated that teeth with larger stresses were at risk of root absorption during the process of pushing and grinding teeth to the far centre by the invisible aligner.

However, when using the invisible aligner to move the molar 0.3 mm, the stress on the second molar by the PDL was more than 26 kPa, which may damage the PDL and cause irreversible necrosis. Therefore, it was not recommended to use the invisible aligner to move the molar by a distance of 0.3 mm.

To analyse the relationship between the movement of the tooth and the pressure-tensile stress of the PDL, the principal stress distributions of the first and second molars were considered. As shown in Fig. 4, tooth movement in the direction of the applied load compressed the PDL on one side and stretched it on the opposite side. According to the "pressure tension" theory [1], bone apposition and resorption occur on PDL's tension and compression sides. This led to the formation of symmetric zones of compression and tension in the periodontium, with compression leading to bone resorption and tension causing bone formation. Therefore, for patients with periodontitis whose alveolar bone was absorbed into half of the root, due to the significant instantaneous stress on the PDL caused by the process of removing and wearing the appliance, patients with moderate to severe periodontitis should be cautious in using invisible appliances. Mild periodontitis patients may experience pathological alveolar bone resorption due to excessive stress applied by invisible appliances. During clinical application, the patient's PDL health should be observed at all times [9].

Orthodontic tooth movement

The results of the tooth movement behaviour of the two models showed that the maxillary second molar had a similar displacement distribution in the same region as the first molar, which was similar to the results of Yokoi's study [35]. The displacement of the first molar was smaller than that of the second molar, and the displacement was in the opposite direction. This result was consistent with the stress distribution of the PDL. In addition, the rotational direction of the first molar was opposite to that of the second molar, and the size of the rotation was slightly smaller. The results for the rotational angle can be concluded as follows. The aligner caused the tooth to rotate in the direction of migration. The rotations in the lingual and buccal directions were almost 0°. The numerical value of the angle increased with migration distance. Orthodontic tooth movement by an invisible aligner was accompanied by the opposite movement of adjacent teeth.

In the process of orthodontic treatment, it is generally considered that except for the teeth to be moved, other teeth are anchored teeth. The stress magnitude and direction are different for each tooth. When the invisible aligner pushes the molars to move distally, in addition to the greater stress on the distal second molars, the ipsilateral maxillary first molars and central incisors were under greater stress. At the same time, the compressive stress on the lingual surface of the

canine and incisor roots was greater than that on the labial surface, which made the maxillary anterior teeth tend to move to the labial side. Therefore, when the molars were pushed distally with clear aligners, it is necessary to evaluate the thickness of the labial bone plate in the anterior region before orthodontics [32]. If the labial bone plate in the anterior tooth area was weak, micro-implant anchorage should be used prophylactically to enhance the anterior tooth area anchorage, control the position of the anterior tooth root, and prevent the labial bone plate from moving to the labial side of the tooth. If the anterior crown was tilted, the second type of traction should be used prophylactically to control the position of the crown and prevent the anterior crown from becoming aggravated during the process of pushing the molars to the distal end.

Behaviour of the invisible aligner

The maximum equivalent stress occurred at the interface of the first and second molars. In the process of wearing the clinical aligner, it was relatively difficult to put the interface in place. Under the double effects of long-term immersion in the mouth and repeated removal and wearing by patients, the aligner was prone to deformation or fracture at the interface between adjacent teeth.

5. Conclusions

In this study, the comparison between aligners with migration displacements of 0.2 mm and 0.3 mm showed similar biomechanical behaviour. The invisible aligner affected not only the displacement and rotation of the orthodontic teeth but also the movement of adjacent teeth. If the migration displacement of the invisible aligner is too large, then it may damage PDL. Therefore, the displacement of the invisible aligner should be considered in addition to the morphology in future applications.

Ethics approval and consent to participate

Human maxillary bone and tooth data were involved in the study. The experimental protocol was established according to the ethical guidelines of the Declaration of Helsinki and was approved by the Ethics Committee of Drugs (Device) of China–Japan Friendship Hospital. Written informed consent was obtained from all subjects.

Availability of data and materials

The datasets used and analysed during the current study available from the corresponding author on reasonable request.

Competing interests

The authors confirm that there is no conflict of interest in relation to this work.

Funding

National Key R&D Program of China (No. 2016YFB1101503).

Acknowledgements

This work was supported by the National Key R&D Program of China (No. 2016YFB1101503).

References

[1] ASIRY M.A., *Biological aspects of orthodontic tooth movement: A review of literature*, Saudi J. Biol. Sci., 2018, 25, 1027–1032.

[2] BARONE S., PAOLI A., RAZIONALE A.V., SAVIGNANO R., *Computer aided modelling to simulate the biomechanical behaviour of customised orthodontic removable appliances*, Int. J. Interact. Des. Manuf., 2016, 10, 387–400.

[3] BENAZZI S., KULLMER O., GROSSE I.R., WEBER G.W., *Brief communication: comparing loading scenarios in lower first molar supporting bone structure using 3D finite element analysis*, Am. J. Phys. Anthropol., 2012, 147, 128–134.

[4] CABALLERO G.M., CARVALHO F.O.A., HARGREAVES B.O., ARAÚJO H.H., JÚNIOR P.A.A.M., OLIVEIRA D.D., *Mandibular canine intrusion with the segmented arch technique: A finite element method study*, Am. J. Orthod. Dentofac. Orthop., 2015, 147, 691–697.

[5] CAI Y., YANG X., HE B., YAO J., *Finite element method analysis of the periodontal ligament in mandibular canine movement with transparent tooth correction treatment*, BMC Oral Health, 2015, 15, 1–11.

[6] CATTANEO P.M., DALSTRA M., MELSEN B., *Moment-to-force ratio, center of rotation, and force level: A finite element study predicting their interdependency for simulated orthodontic loading regimens*, Am. J. Orthod. Dentofac. Orthop., 2008, 133, 681–689.

[7] COMBA B., PARRINI S., ROSSINI G., CASTROFLORIO T., DEREGIBUS A., *A three-dimensional finite element analysis of upper-canine distalization with clear aligners, composite attachments, and class II elastics*, J. Clin. Orthod., 2017, 51, 24–28.

[8] ELKHOLY F., MIKHAIEL B., SCHMIDT F., LAPATKI B.G., *Mechanical load exerted by PET-G aligners during mesial and distal derotation of a mandibular canine: An in vitro study*, J. Orofac. Orthop., 2017, 78, 1–9.

[9] FONTANA M., COZZANI M., CAPRIOGLIO A., *Soft tissue, skeletal and dentoalveolar changes following conventional anchorage molar distalization therapy in class II non-growing subjects: a multicentric retrospective study*, Prog. Orthod., 2012, 13, 30–41.

[10] GOMEZ J.P., PEÑA F.M., MARTÍNEZ V., GIRALDO D.C., CARDONA C.I., *Initial force systems during bodily tooth movement with plastic aligners and composite attachments: A three-dimensional finite element analysis*, Angle Orthod., 2015, 85, 454–460.

[11] GRÖNING F., BRIGHT J.A., FAGAN M.J., O'HIGGINS P., *Improving the validation of finite element models with quantitative full-field strain comparisons*, J. Biomech., 2012, 45, 1498–1506.

[12] GRÖNING F., FAGAN M., O'HIGGINS P., *Modeling the Human Mandible Under Masticatory Loads: Which Input Variables are Important?*, Anat. Rec., 2012, 295, 853–863.

[13] GUPTA M., MADHOK K., KULSHRESTHA R., CHAIN S., KAUR H., YADAV A., *Determination of stress distribution on periodontal ligament and alveolar bone by various tooth movements–A 3D FEM study*, J. Oral Biol. Craniofac. Res., 2020, 10, 758–763.

[14] HAHN W., ZAPF A., DATHE H., FIALKA-FRICKE J., FRICKE--ZECH S., GRUBER R., SADAT-KHONSARI R., *Torquing an upper central incisor with aligners – acting forces and biomechanical principles*, Eur. J. Orthod., 2010, 32, 607–613.

[15] HERAVI F., SALARI S., TANBAKUCHI B., LOH S., AMIRI M., *Effects of crown-root angle on stress distribution in the maxillary central incisors' PDL during application of intrusive and retraction forces: a three-dimensional finite element analysis*, Prog. Orthod., 2013, 14, 1–10.

[16] HEDAYATI Z., SHOMALI M., *Maxillary anterior en masse retraction using different antero-posterior position of mini screw: a 3D finite element study*, Prog. Orthod., 2016, 17, 1–7.

[17] HOHMANN A., KOBER C., YOUNG P., DOROW C., GEIGER M., BORYOR A., SANDER F.G., *Influence of different modeling strategies for the periodontal ligament on finite element simulation results*, Am. J. Orthod. Dentofac. Orthop., 2011, 139, 775–783.

[18] HOHMANN A., WOLFRAM U., GEIGER M., BORYOR A., SANDER C., FALTIN R., SANDER F.G., *Periodontal Ligament Hydrostatic Pressure with Areas of Root Resorption after Application of a Continuous Torque Moment*, Angle Orthod., 2007, 77, 653–659.

[19] HOHMANN A., WOLFRAM U., GEIGER M., BORYOR A., KOBER C., SANDER C., SANDER F.G., *Correspondences of hydrostatic pressure in periodontal ligament with regions of root resorption: A clinical and a finite element study of the same human teeth*, Comput. Meth. Prog. Bio., 2009, 93, 155–161.

[20] KOJIMA Y., FUKUI H., *Numerical simulations of canine retraction with T-loop springs based on the updated moment-to-force ratio*, Eur. J. Orthod., 2012, 34, 10–18.

[21] KRISHNAN V., DAVIDOVITCH Z., *Cellular, molecular, and tissue-level reactions to orthodontic force*, Am. J. Orthod. Dentofac. Orthop., 2006, 129, 469.e1–469.e32.

[22] KUO E., MILLER R.J., *Automated custom-manufacturing technology in orthodontics*, Am. J. Orthod. Dentofac. Orthop., 2003, 123, 578–581.

[23] LI Y., JACOX L.A., LITTLE S.H., KO C.C., *Orthodontic tooth movement: The biology and clinical implications*, Kaohsiung J. Med. Sci., 2018, 34, 207–214.

[24] LIMBERT G., MIDDLETON J., *A compressible transversely isotropic hyperelastic constitutive law for modelling the periodontal ligament: analytical and computational aspects*, Acta. Bioeng. Biomech., 2003, 4, 137–138.

[25] NIKOLAUS A., CURREY J.D., LINDTNER T., FLECK C., ZASLANSKY P., *Importance of the variable periodontal ligament geometry for whole tooth mechanical function: a validated numerical study*, J. Mech. Behav. Biomed. Mater., 2017, 67, 61–73.

[26] NYASHIN Y.I., NYASHIN M.Y., *Biomechanical modelling of periodontal ligament behaviour under various mechanical loads*, Acta. Bioeng. Biomech., 2000, 2, 67–74.

[27] PROVATIDIS C.G., *A comparative FEM-study of tooth mobility using isotropic and anisotropic models of the periodontal ligament*, Med. Eng. Phys., 2000, 22, 359–370.

[28] REINOSO M.R., CIVERA M., BURGIO V., BERGAMIN F., RUIZ O.G., PUGNO N.M., SURACE C., *3D printing and testing of rose thorns or limpet teeth inspired anchor device for tendon tissue repair*, Acta. Bioeng. Biomech., 2021.

[29] SARKAR S., SAHU T.P., DATTA A., CHANDRA N., CHAKRABORTY A., DATTA P., CHOWDHURY A.R., *Mechanical response at peri-implant mandibular bone for variation of pore characteristics of implants: A Finite Element Study*, Acta. Bioeng. Biomech., 2019, 21.

[30] TANNE K., NAGATAKI T., INOUE Y., SAKUDA M., BURSTONE C.J., *Patterns of initial tooth displacements associated with various root lengths and alveolar bone heights*, Am. J. Orthod. Dentofac. Orthop., 1991, 100, 66–71.

[31] TURPIN D.L., *Clinical trials needed to answer questions about Invisalign*, Am. J. Orthod, Dentofacial Orthop., 2005, 127, 157–158.

[32] VARDIMON A.D., OREN E., BEN-BASSAT Y., *Cortical bone remodeling/tooth movement ratio during maxillary incisor retraction with tip versus torque movements*, Am. J. Orthod. Dentofac. Orthop., 1998, 114, 520–529.

[33] WANG D., AKBARI A., JIANG F., LIU Y., CHEN J., *The effects of different types of periodontal ligament material models on stresses computed using finite element models*, Am. J. Orthod. Dentofac. Orthop., 2022, 162, e328–e336.

[34] WEIR T., *Clear aligners in orthodontic treatment*, Aust. Dent. J., 2017, 62, 58–62.

[35] YOKOI Y., ARAI A., KAWAMURA J., UOZUMI T., USUI Y., OKAFUJI N., *Effects of Attachment of Plastic Aligner in Closing of Diastema of Maxillary Dentition by Finite Element Method*, J. Healthc. Eng., 2019, 1–6.

[36] ZHENG M., LIU R., NI Z., YU Z., *Efficiency, effectiveness and treatment stability of clear aligners: A systematic review and meta-analysis*, Orthod. Craniofac. Res., 2017, 20, 127–133.